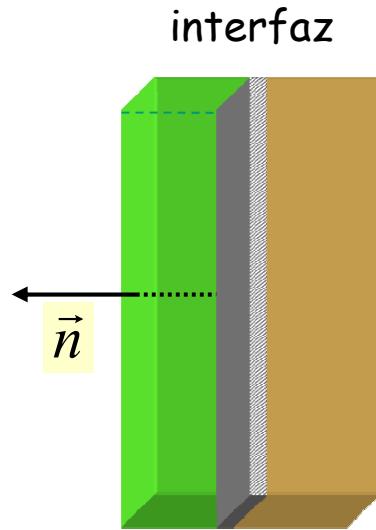


8a Anisotropía de Intercambio

Otros usos: superficies e interfaces

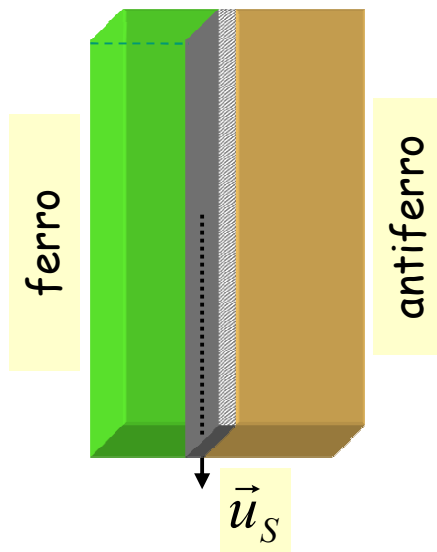
Anisotropía de interfaz



$$e_K = K_S [1 - (\vec{m} \cdot \vec{n})^2]$$

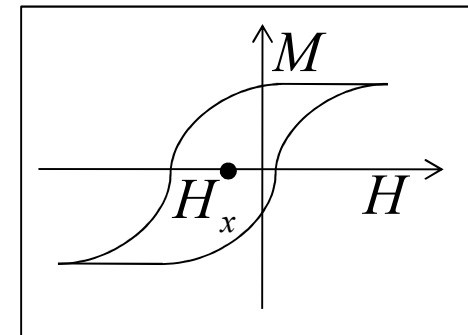
$$\left. \begin{array}{l} K_S > 0 \Rightarrow \vec{m} // \text{sup} \\ K_S < 0 \Rightarrow \vec{m} \perp \text{sup} \end{array} \right\}$$

Anisotropía de intercambio*



$$e_K = K_S \vec{m} \cdot \vec{u}_S = \frac{H_x}{2} \vec{m} \cdot \vec{u}_S$$

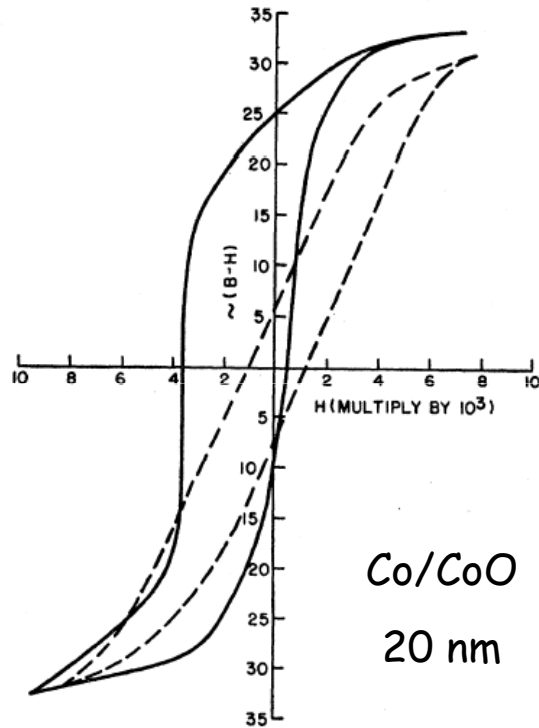
$$e_K = \frac{H_x}{2} m \cos \varphi$$



Exchange bias field

*también llamada unidireccional

Anisotropía de intercambio



Letters to the Editor

New Magnetic Anisotropy

W. H. MEIKLEJOHN AND C. P. BEAN

General Electric Research Laboratory, Schenectady, New York

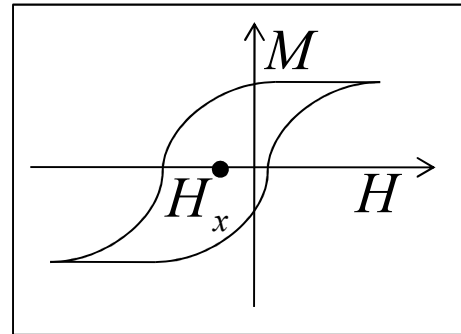
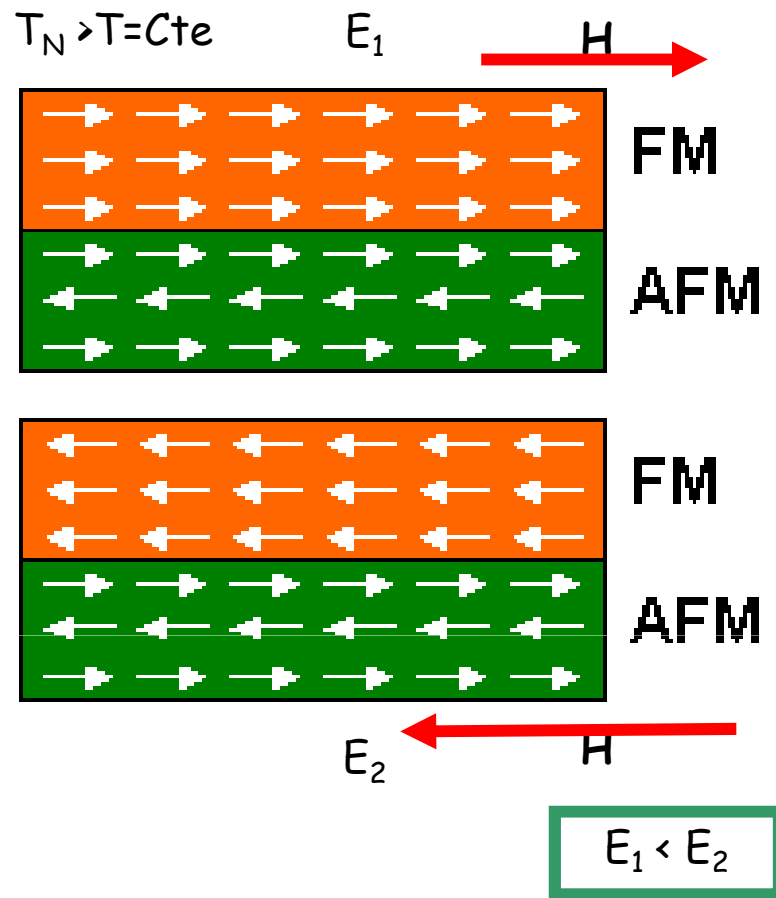
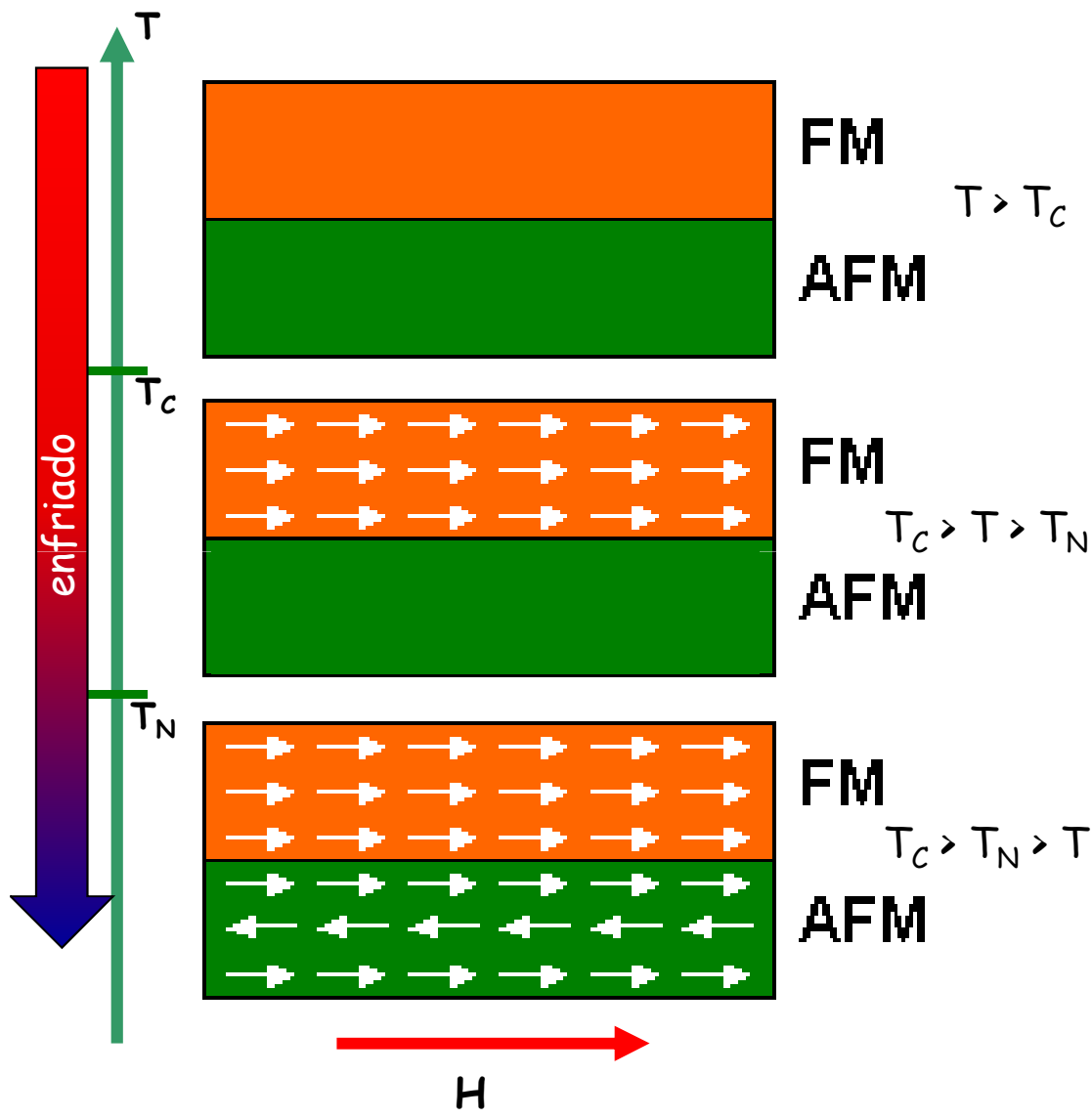
(Received March 7, 1956)

PHYSICAL REVIEW

VOLUME 102, NUMBER 5

JUNE 1, 1956

Anisotropía de intercambio



Anisotropía de intercambio

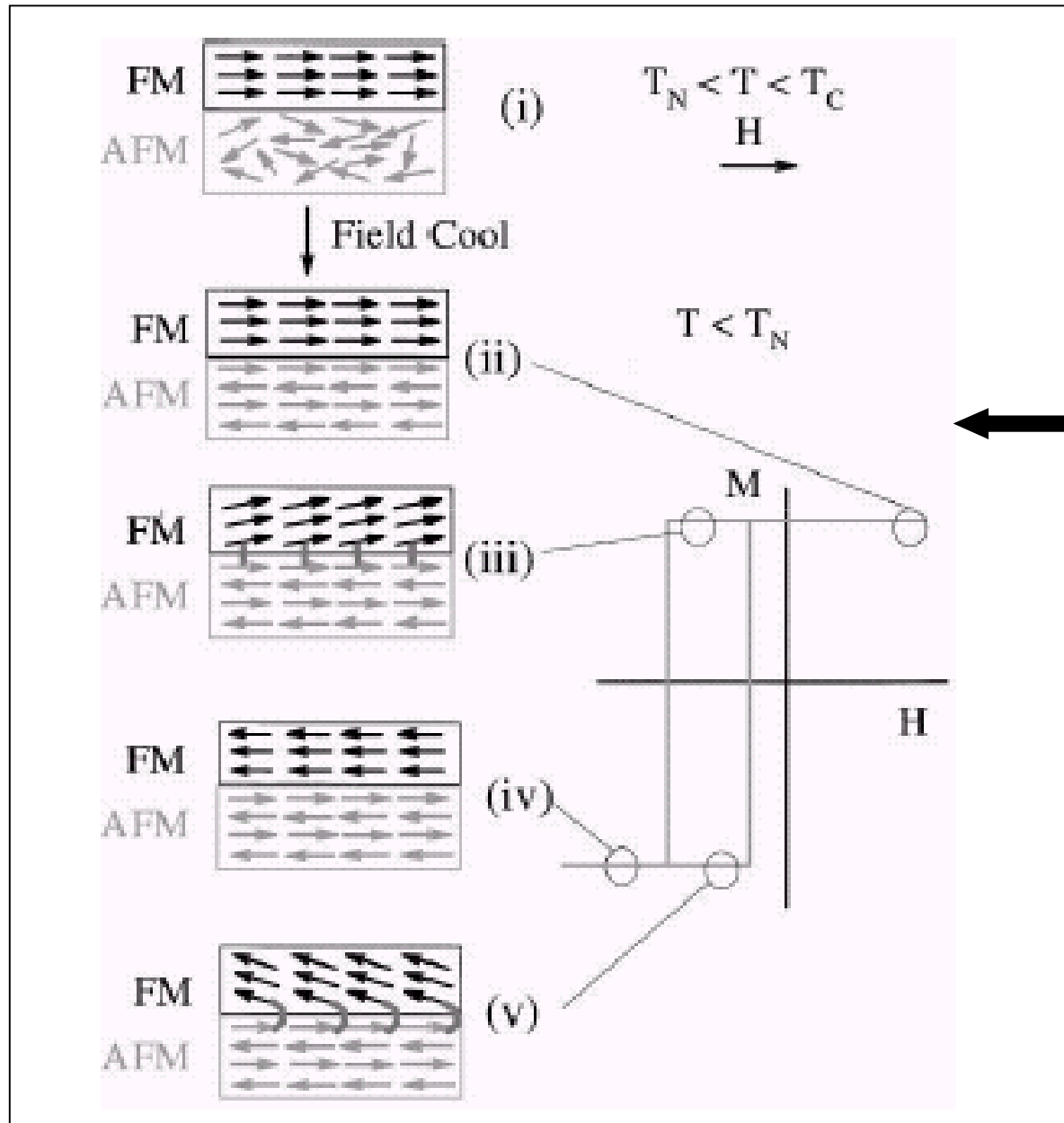
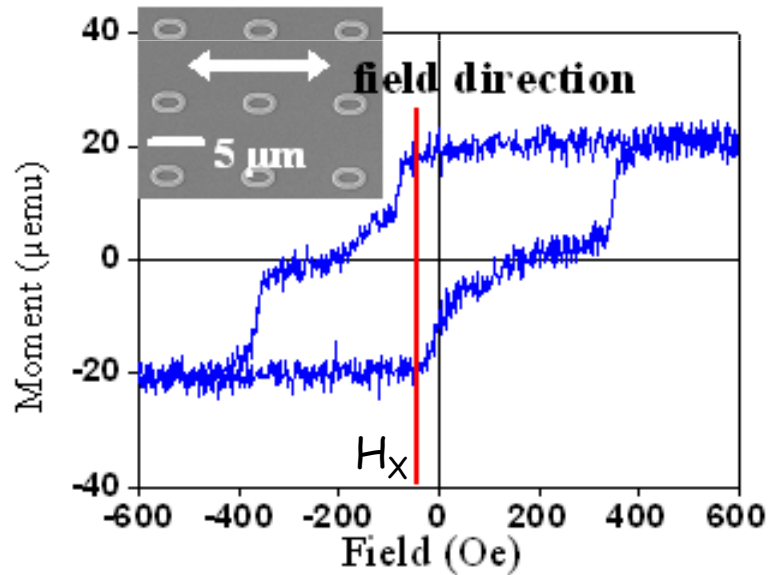
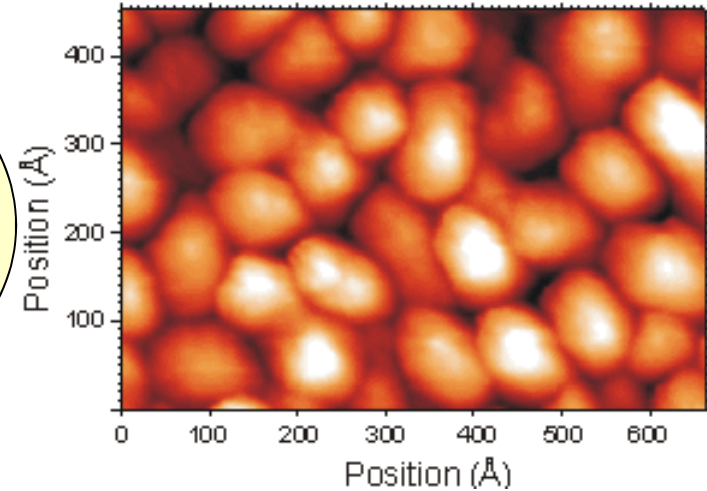
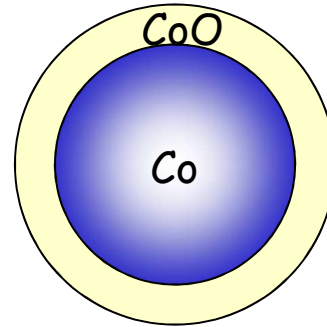


Diagrama esquemático de una configuración de spin FM / AFM.

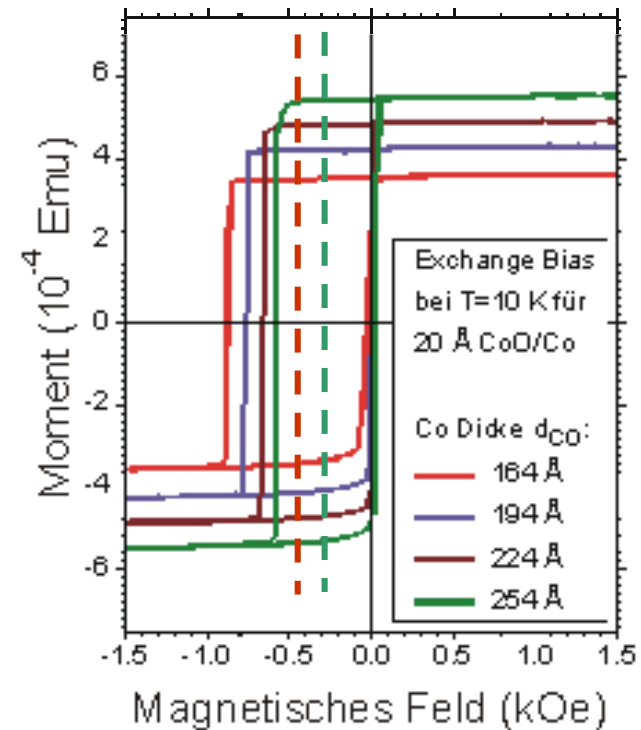
Observación de la anisotropía de intercambio

Exchange bias

CoO/Co



Ta 20nm / NiFe 20nm / FeMn 10 nm film



Exchange Coupling in the Paramagnetic State

J. W. Cai, Kai Liu, and C. L. Chien, *The Johns Hopkins University, Baltimore, MD 21218*

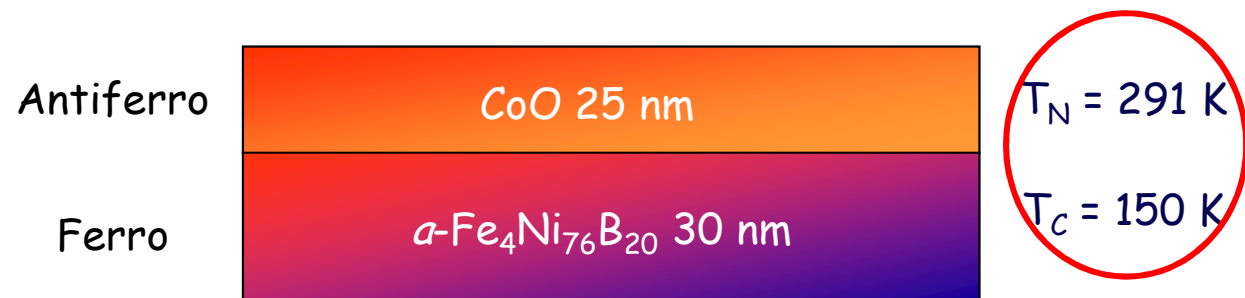
I. Introduction

When a ferromagnet (FM)/ antiferromagnet (AF) bilayer, with the Curie temperature (T_C) of the FM higher than the Néel temperature (T_N) of the AF, has been field-cooled across T_N , an exchange bias is set in. The resultant hysteresis loop of the FM is now shifted by an amount termed the exchange field (H_E), accompanied by an enhanced coercivity (H_C). In the cases thus far reported, T_C has always been much higher than T_N . During field cooling across T_N , the FM layer is in the single-domain state while the exchange coupling is being locked in. It has been generally accepted that $T_C > T_N$ is a prerequisite for establishing FM/AF exchange coupling. In this work, we have studied an FM/AF bilayer of α -Fe₄Ni₇₆B₂₀ ($T_C \sim 150$ K) and CoO ($T_N = 291$ K) with T_C *much lower* than T_N , a hitherto unexplored regime where the FM ordering is absent when the exchange coupling is being established. We have observed exchange coupling in this system, which persists well into the paramagnetic (PM) state ($T > T_C$).

II. Results

The hysteresis loop of a single 300 Å α -Fe₄Ni₇₆B₂₀ layer at 80 K is shown in Fig. 1a, exhibiting a square loop with a small coercivity of only 0.4 Oe, which are characteristics of a soft FM. However, a bilayer of α -Fe₄Ni₇₆B₂₀(300 Å)/CoO (250 Å), field-cooled in a field of 10 kOe to 80 K, shows a shifted hysteresis loop with large values of H_E and H_C , which are clear signatures of exchange coupling. The hysteresis loops measured at successively higher temperature from 80 K to 290 K are shown in Fig. 1c – 1h. At higher temperatures, the coercivity progressively decreases and vanishes near T_C . Most strikingly, the *collapsed* loop at $T > T_C$ continues to be shifted with an exchange field H_E , which first increases to a maximum before decreasing progressively to zero at 290 K, the T_N of CoO. Thus, we not only have observed exchange coupling at $T < T_C$ in a bilayer where T_C is much less than T_N , but also at $T > T_C$, when the FM layer is in the PM state.

Exchange Coupling in the Paramagnetic State



Exchange Coupling in the Paramagnetic State

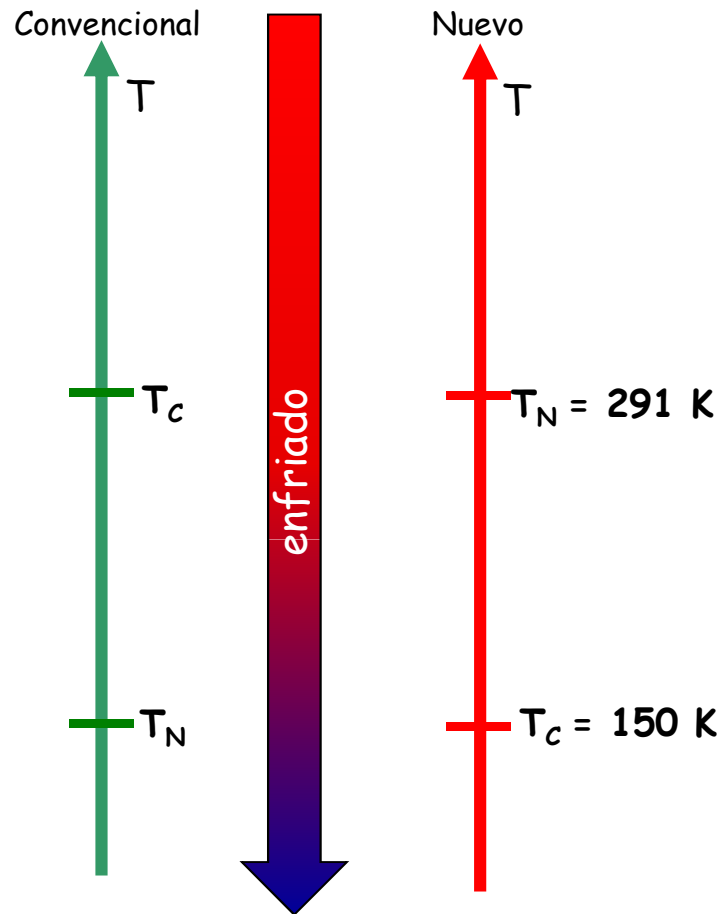
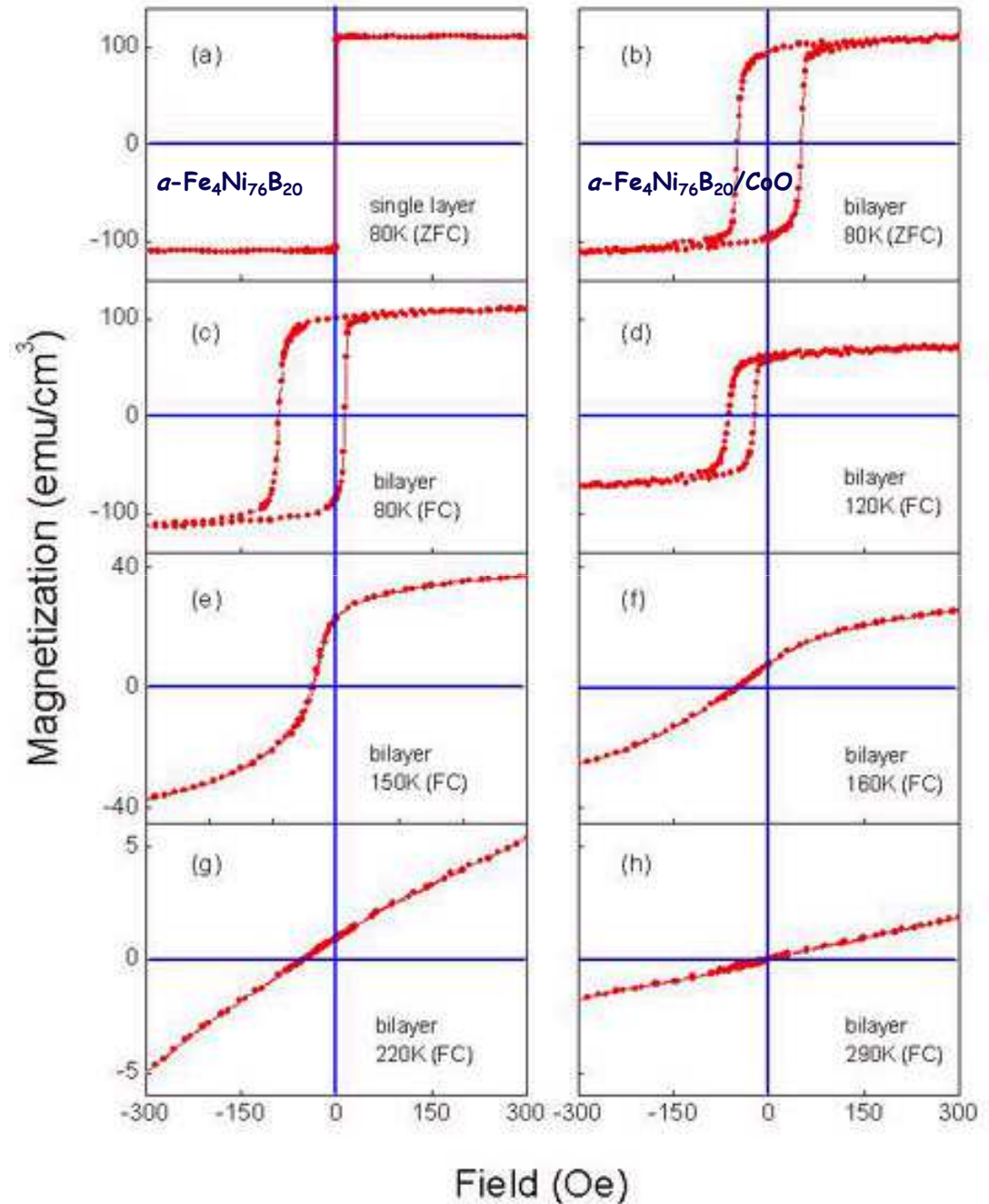


Figure 1: Hysteresis loops of a single layer $\alpha\text{-Fe}_4\text{Ni}_7\text{B}_{20}$ at 80 K (a) and a bilayer of $\alpha\text{-Fe}_4\text{Ni}_7\text{B}_{20}$ (300 Å)/CoO (250 Å) at 80 K after zero-field cooling to 80 K (b), after field cooling in 10 kOe to 80 K and measured at 80 K (c), 120 K (d), 150 K (e), 160 K (f), 220 K (g), and 290 K (h). 0



Exchange Coupling in the Paramagnetic State

The temperature dependence of H_E and H_C , obtained from the hysteresis loops shown in Fig. 1c-1h, are presented in Fig. 2. A number of striking features are evident. First of all, H_E and the enhanced H_C do not both vanish at T_N , completely different from what has been universally observed in bilayers with $T_C > T_N$. Instead, while H_E vanishes at T_N , H_C vanishes at a lower temperature near T_C . This indicates vividly that in exchange-coupled FM/AF bilayers, the exchange field is dictated by the AF ordering, but the coercivity, although significantly enhanced by the exchange coupling, is intrinsic to the FM ordering. Most importantly, the collapsed loop continues to be shifted from $H = 0$ at $T > T_C$, i.e., the exchange coupling persists when the FM layer is already in the PM state. It is noted in Fig. 2 that, while H_C decreases monotonically with temperature and reaches the terminal value at T_C , H_E shows a sharp rise near T_C before decreasing towards zero at T_N .

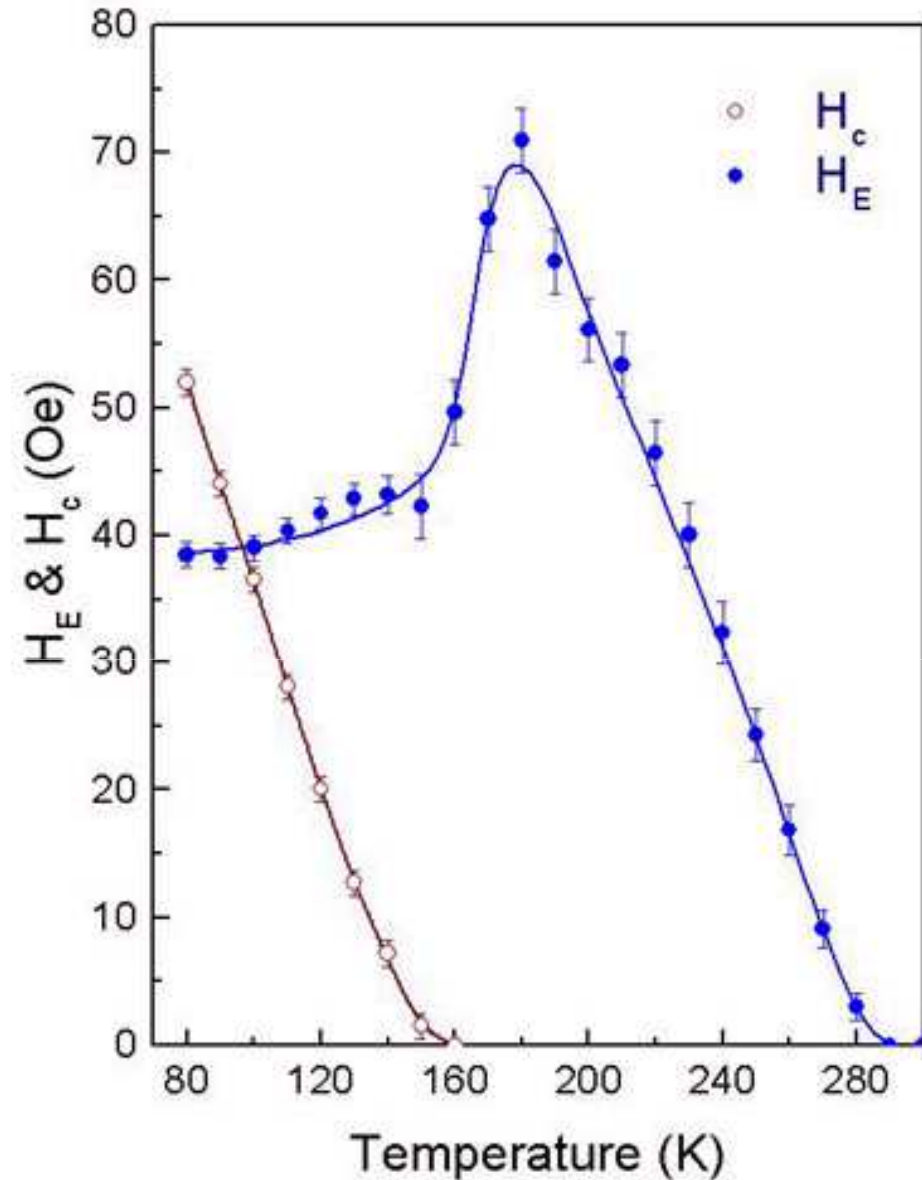


Figure 2: Temperature dependence of exchange field H_E and coercivity H_C of $\alpha\text{-Fe}_4\text{Ni}_{76}\text{B}_{20}(300 \text{ \AA})/\text{CoO}(250 \text{ \AA})$ after field cooling in 10 kOe to 80 K.

Exchange Coupling in the Paramagnetic State

The realization of exchange coupling in bilayers with $T_C \ll T_N$ also has important implication in technological application of exchange coupling in spin-valve devices. For FM/AF bilayers with optimized performance, one can broaden the search to a greater variety of FM and AF materials to realize suitable values of H_E and H_C near room temperature without regard to the condition of $T_C > T_N$.

III. Summary

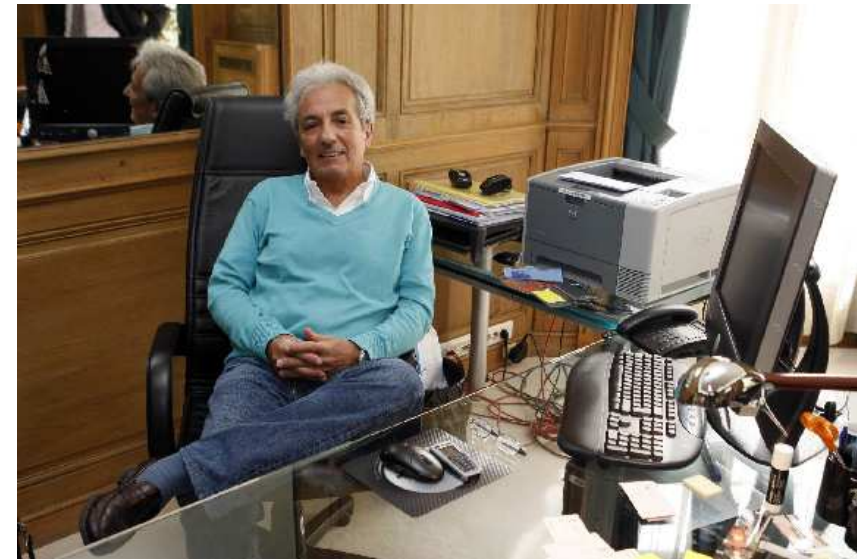
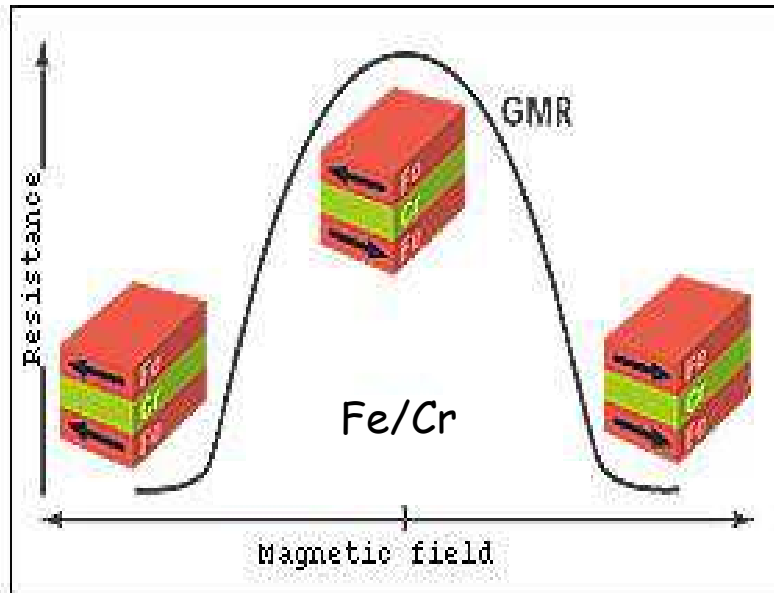
Contrary to the common perception of $T_C > T_N$ as a prerequisite for exchange coupling between a FM and an AF layers, we have demonstrated exchange coupling where $T_C \ll T_N$. The exchange coupling exists not only in $T < T_C$, but also in $T_C < T < T_N$, where the bulk of the FM layer is in the PM state. With increasing temperature, H_C vanishes at T_C , whereas H_E persists to T_N . The results show that the exchange coupling can be established in FM/AF bilayers regardless of the relative values of T_C and T_N .

Reference

J. W. Cai, Kai Liu, and C. L. Chien, Phys. Rev. B 60, 72 (1999).

Anisotropía de intercambio - válvula de spin

Magneto-resistencia gigante



Albert Fert, Nobel Prize in Physics 2007

Giant Magnetoresistance of (001) Fe/(001) Cr Magnetic Superlattices

M. N. Baibich,^(a) J. M. Broto, A. Fert, F. Nguyen Van Dau, and F. Petroff
Laboratoire de Physique des Solides, Université Paris-Sud, F-91405 Orsay, France

P. Eitenne, G. Creuzet, A. Friederich, and J. Chazelas
Laboratoire Central de Recherches, Thomson CSF, B.P. 10, F-91401 Orsay, France
(Received 24 August 1988)

PHYSICAL REVIEW LETTERS

VOLUME 61, NUMBER 21

21 NOVEMBER 1988

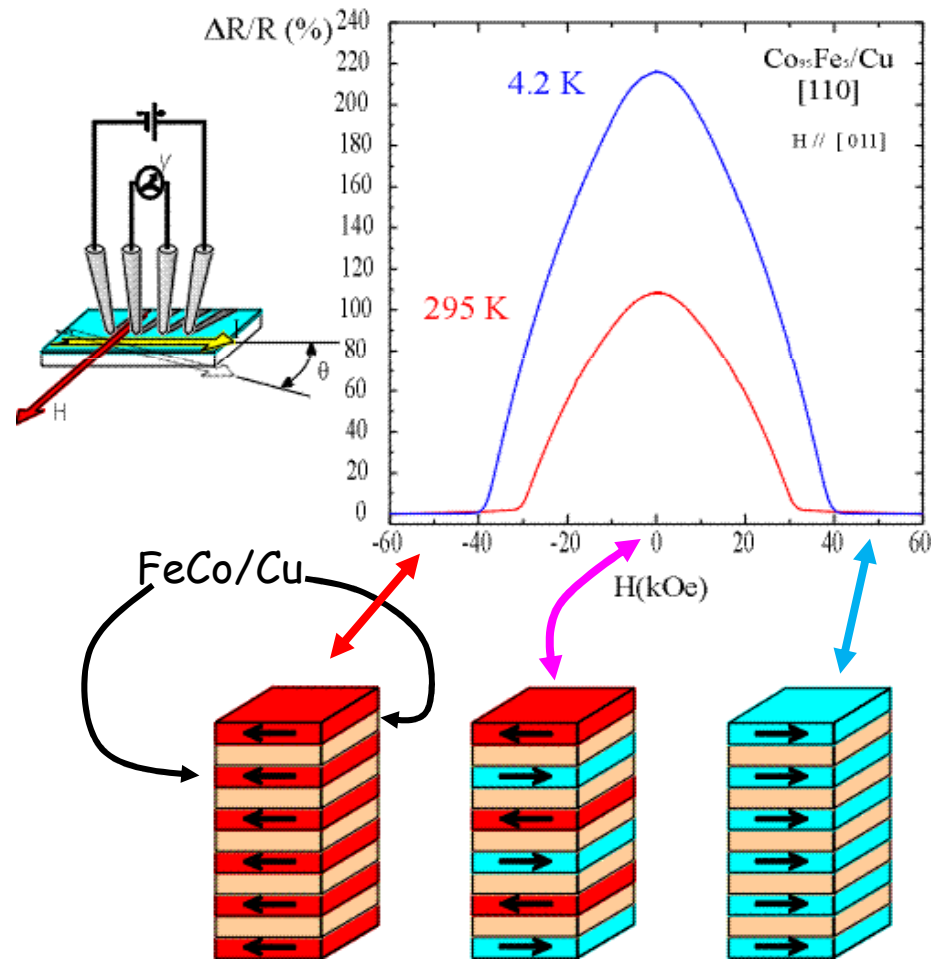


Peter Grünberg, Nobel Prize in Physics 2007

Anisotropía de intercambio - válvula de spin

Magneto-resistencia gigante

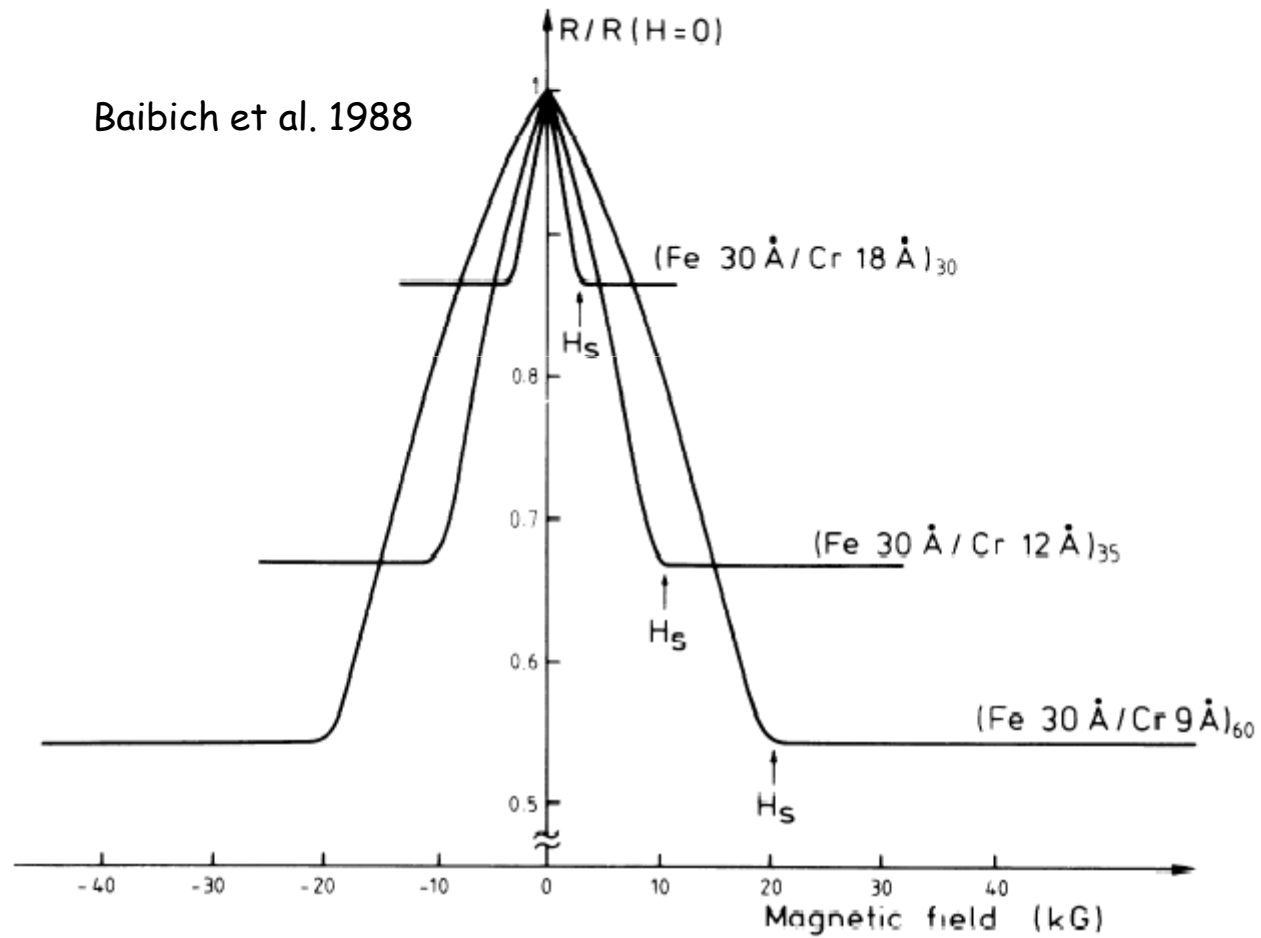
Giant Magnetoresistance



Anisotropía de intercambio - válvula de spin

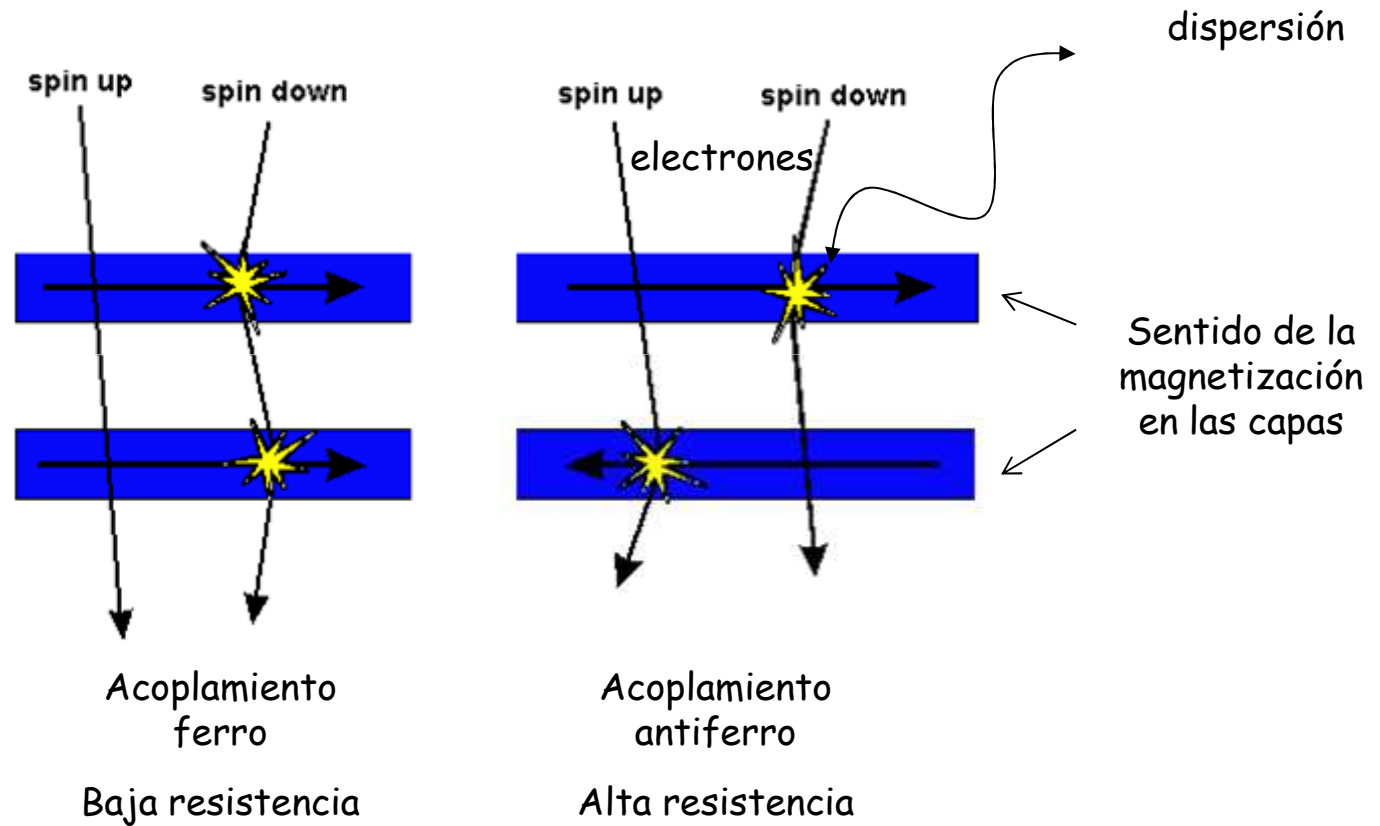
Magnetoresistencia gigante

Resultados experimentales



Anisotropía de intercambio - válvula de spin

Magneto-resistencia gigante



Anisotropía de intercambio - válvula de spin

Magneto-resistencia gigante

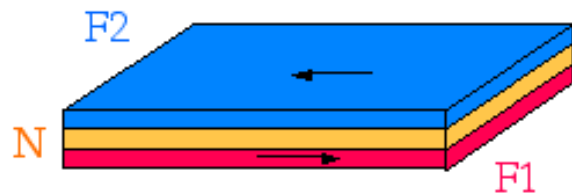
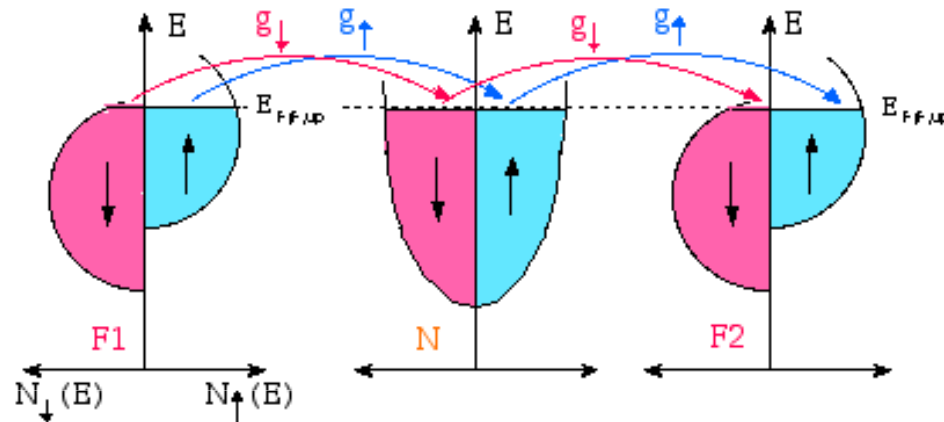
Magneto-resistance - spin valve

$$g \propto N(E_F)$$

F1 and F2 **parallel**:

$g_{\uparrow} > g_{\downarrow}$
 g_{\uparrow} dominates

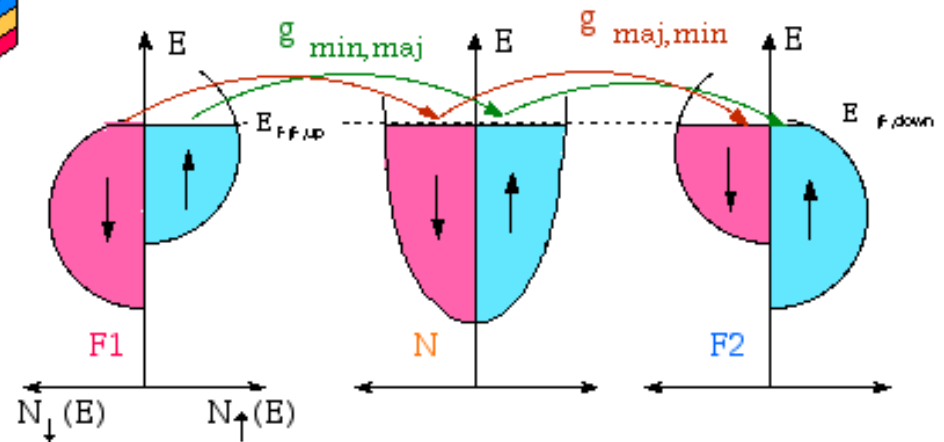
Low R state



F1 and F2 **antiparallel**:

$g_{\min, \text{maj}} = g_{\text{maj}, \min} < g_{\uparrow}$

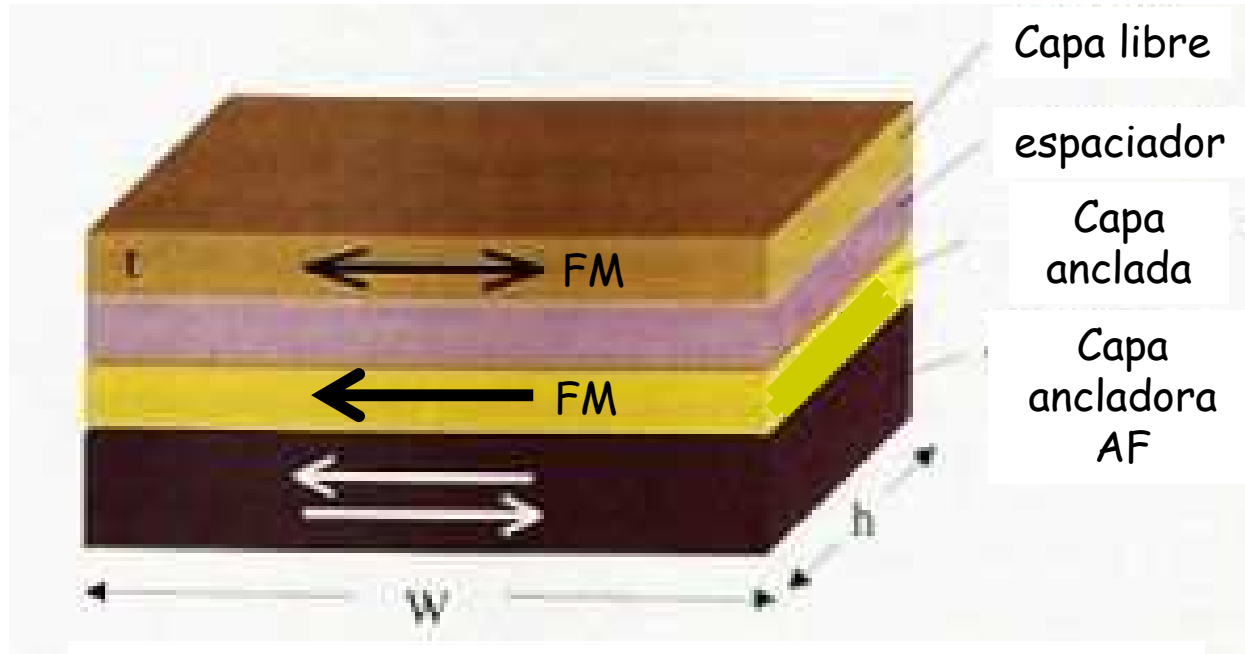
High R state



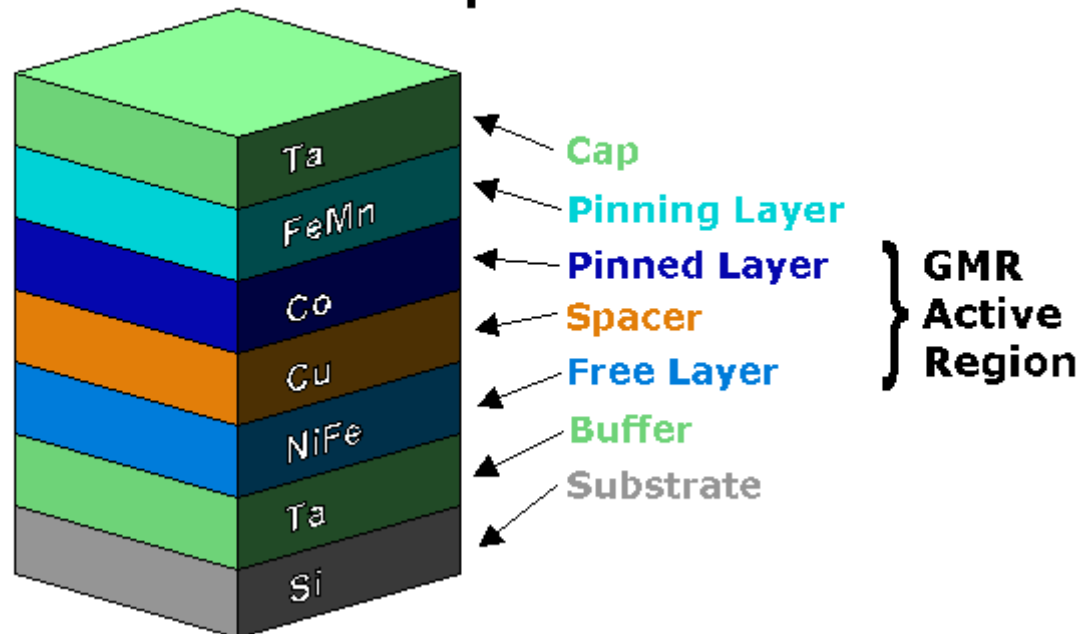
Grunberg PRB (89), Fe/Cr spin valve MR=1.5%

Baibich et al., PRL (88), Fe/Cr multilayer

Anisotropía de intercambio - válvula de spin

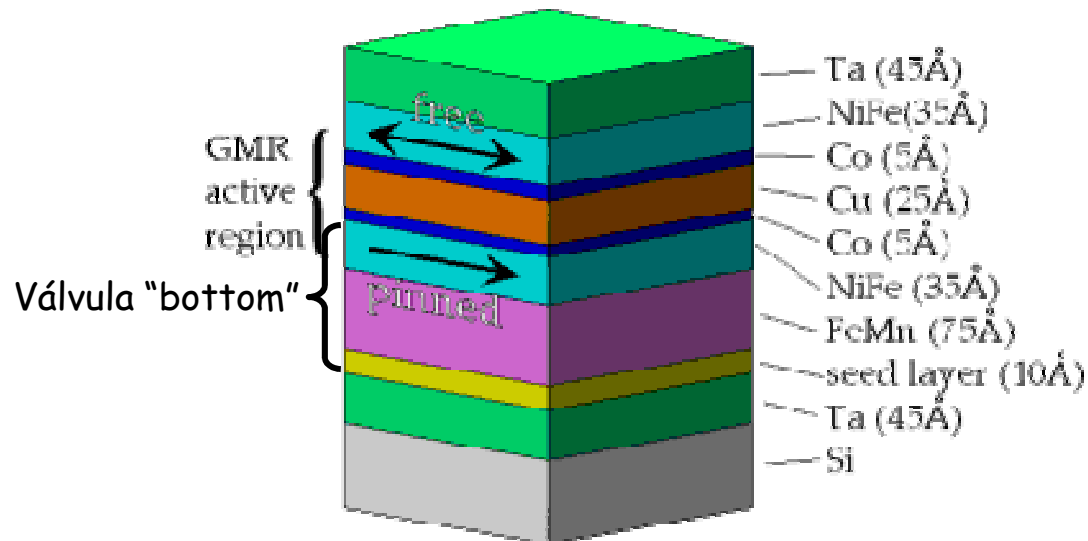
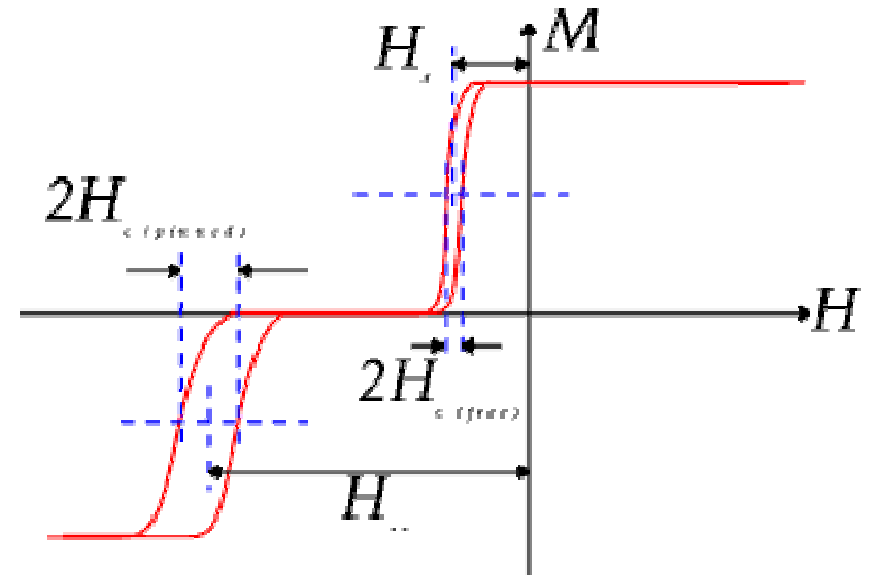
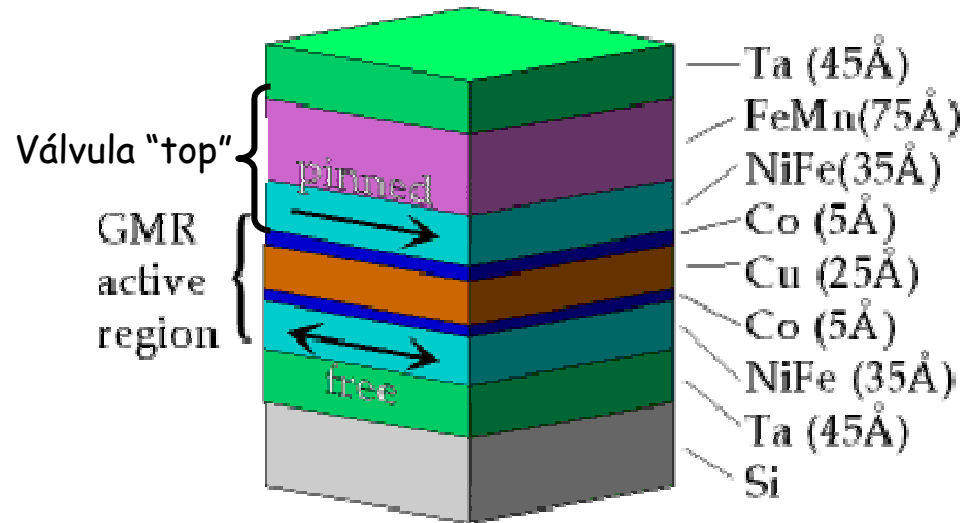


Spin Valve Structure



Magnetoresistencia y válvulas de spin - adenda

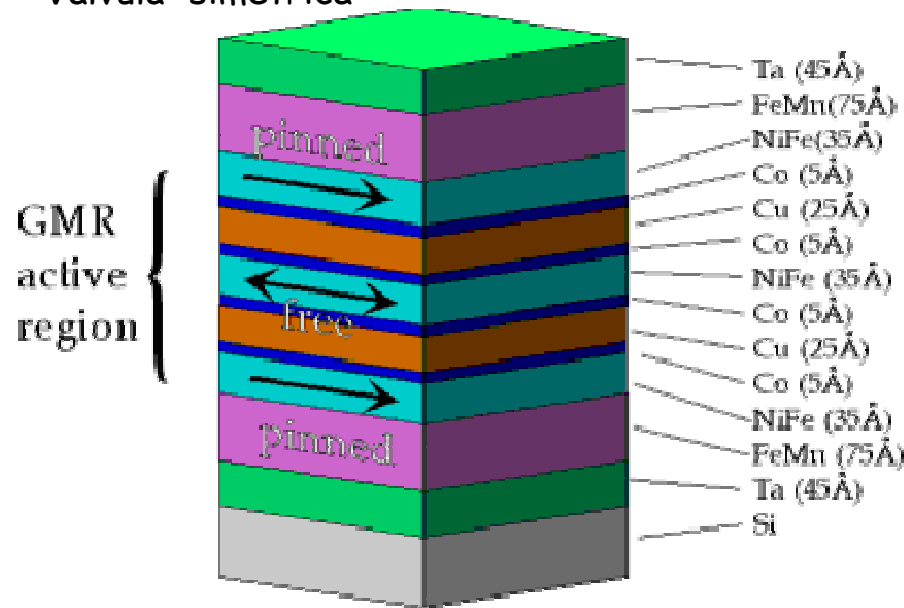
Válvulas de spin



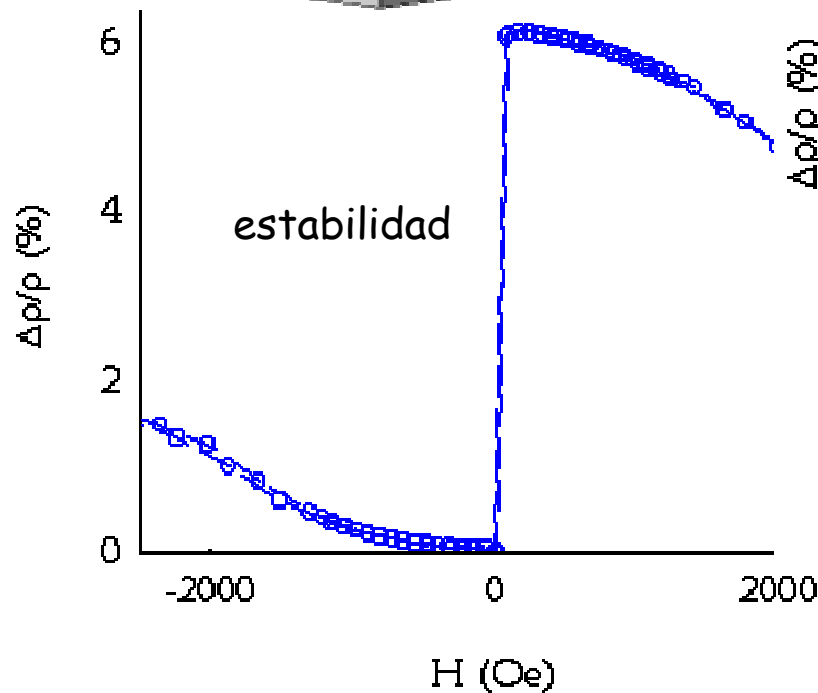
Magnetoresistencia y válvulas de spin - adenda

Válvula "simétrica"

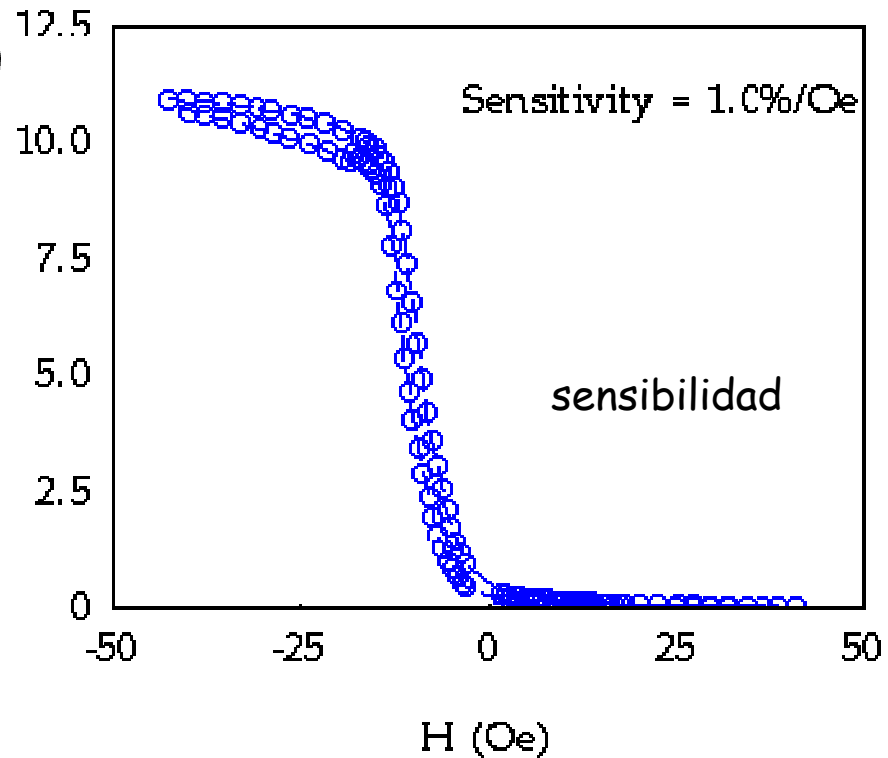
Válvulas de spin



GMR active region



Symmetric Spin-valve minor loop

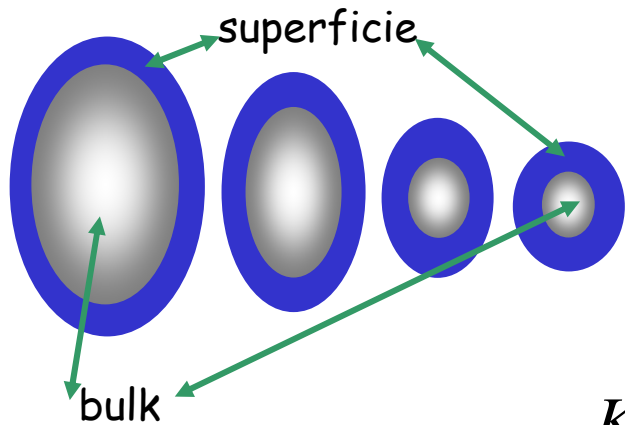


[animación](#)

Anisotropía de Superficie en Nanopartículas

Partículas ferromagnéticas pequeñas - efectos dinámicos

Anisotropía de superficie



Las superficies/interfaces presentan características especiales. Existe una discontinuidad composicional y configuracional, lo cual modifica las propiedades magnéticas. Se ha observado un **mayor efecto anisotrópico** en las superficies libres, frecuentemente con dirección radial. Por otro lado se ha observado una tendencia a menores efectos de intercambio en los átomos "superficiales" lo cual favorece el comportamiento paramagnético en esa región, incluso es frecuente la referencia a una capa superficial magnéticamente "muerta".

$$K_{ef} = K_B + K_{V_S}^{ef}$$

$$K_{V_S}^{ef} \approx \frac{SK_S}{V} \approx \frac{4\pi r^2}{\frac{4}{3}\pi r^3} K_S = \frac{3}{r} K_S = \frac{6}{d} K_S \quad \text{Partícula esférica}$$

$K_S = 10^4 - 10^3 \text{ J/m}^2$,
energía de anisotropía por
unidad de área superficial

$$K_{ef} = K_B + \frac{6K_S}{d}$$

$$K_{ef} = K_B + \gamma \frac{K_S}{d}$$

Bødker et. Al (1994)

¿Efecto de
distribución de
tamaños de
partículas?

Partículas ferromagnéticas pequeñas - efectos dinámicos

Anisotropía de superficie - ejemplo

$$K_B(\text{Co}_{fcc}) \approx 1 \times 10^5 \text{ J / m}^3$$

$$K_S(\text{Co / Al}_2\text{O}_3) \approx 3.3 \times 10^{-4} \text{ J / m}^2$$

$$K_{ef} = K_B + \gamma \frac{K_s}{d}$$

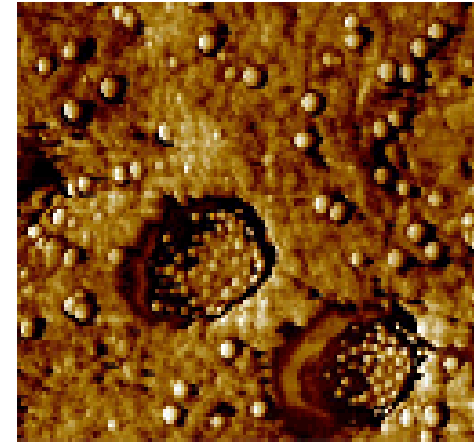


imagen MFA de nanopartículas de Co fcc en una matriz de alúmina. Las partículas son de aprox. 11 nm (diámetro).

$$K_{ef}(\text{Co / Al}_2\text{O}_3) \approx \left[1 \times 10^5 + 6 \frac{3.3 \times 10^{-4}}{11 \times 10^{-9}} \right] \text{ J / m}^3 \approx 2.8 \times 10^5 \text{ J / m}^3$$

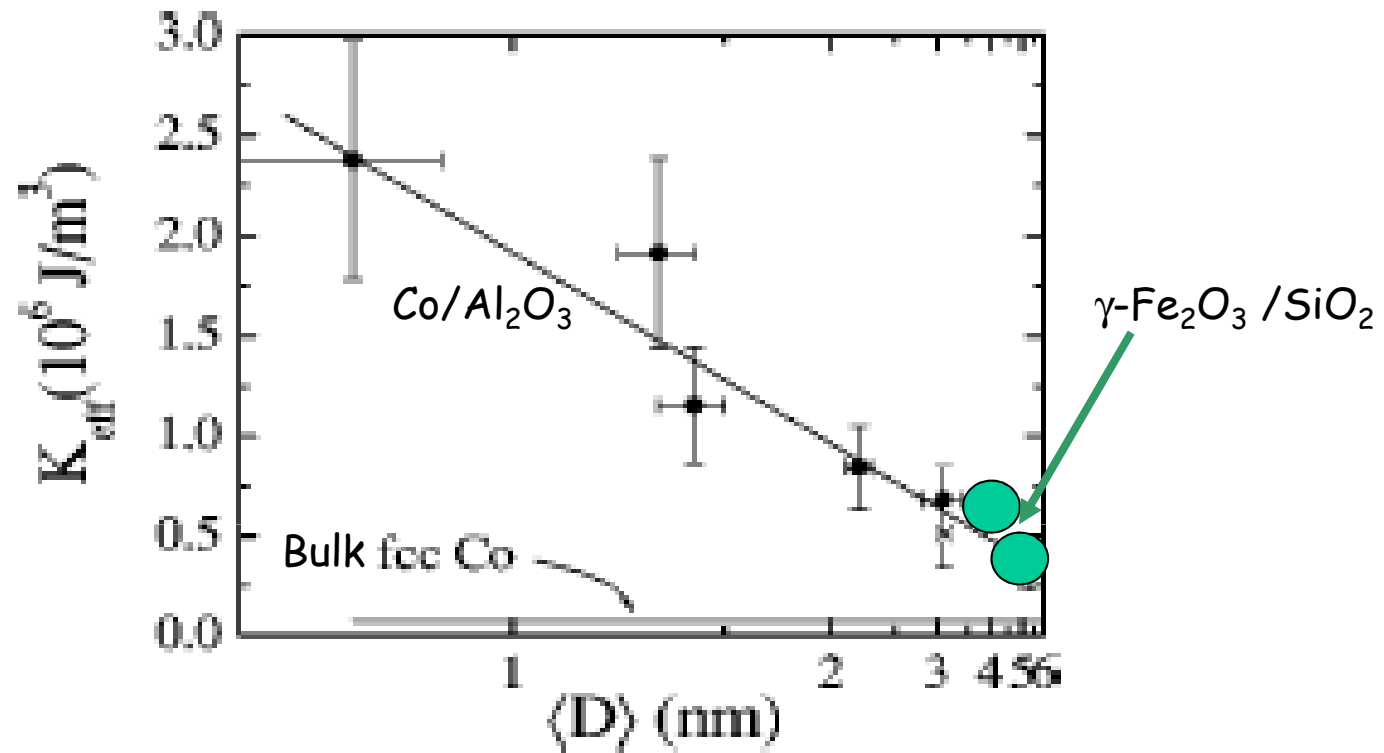
Si $d \sim 3 \text{ nm} = 3 \times 10^{-9} \text{ m}$

$$\longrightarrow K_{ef}(\text{Co / Al}_2\text{O}_3) \approx 10^6 \text{ J / m}^3$$

$$\tau = \tau_0 e^{\frac{K_{ef} V}{kT}}$$

Mayores tiempos de relajación

Partículas ferromagnéticas pequeñas - efectos dinámicos



F. Luis, J.M. Torres, L.M. Gracia, J. Bartolomé, J. Stankiewicz, F. Petroff, F. Fettar, J. L. Maurice and A. Vaurés. Phys. Rev B, **65** (2002) 094409